nutrients

MDPI

Article

Lactiplantibacillus plantarum CCNH185 Alleviates Hyperuricemia by Regulating Nucleoside Degradation, Uric Acid Metabolism and Intestinal Microflora

Yifan Niu [1], Chengfei Fan [2], Zhengyuan Zhai [3], Juan Yang [4], Jiahao Huang [4], Xiaowei Zheng [4,*] and Yanling Hao [1,*]

[1] Food Laboratory of Zhongyuan, Henan University of Technology, Zhengzhou 450001, China
[2] Key Laboratory of Precision Nutrition and Food Quality, Department of Nutrition and Health, China Agricultural University, Beijing 100193, China
[3] College of Food Science and Nutritional Engineering, China Agricultural University, Beijing 100083, China
[4] Nutrition & Health Research Institute, COFCO Corporation, Beijing 102209, China
* Correspondence: zhengxiaowei@cofco.com (X.Z.); haoyl@cau.edu.cn (Y.H.)

Abstract

Background/Objectives: Hyperuricemia (HUA) is a metabolism-related condition resulting from impaired purine metabolism. This study evaluated the alleviating effects of *Lactiplantibacillus plantarum* CCNH185, a strain with high inosine and guanosine degradation activity, in HUA mice. Methods: Fifteen L. plantarum strains were screened for nucleoside degradation in vitro via HPLC. HUA mice, induced by potassium oxonate, inosine, and guanosine, were treated with CCNH185. Hepatic UA synthesis enzymes, renal/intestinal UA transporters, intestinal barrier, inflammation, serum metabolites, and gut microbiota were assessed. Results: CCNH185 alleviated the HUA phenotype and inhibited hepatic UA synthesis enzymes. It decreased the UA reabsorption protein *GLUT9* and increased the excretory transporter *ABCG2* in the kidney and intestine. CCNH185 also restored intestinal barrier integrity and reduced pro-inflammatory cytokines in the intestine and liver. Metabolomics showed reduced serum inosine. Furthermore, CCNH185 promoted Lactiplantibacillus and Akkermansia while inhibiting Clostridium difficile and Turicimonas muris, improving gut microbiota. Conclusions: *L. plantarum* CCNH185 alleviates HUA through multiple pathways, including regulating uric acid synthesis and excretion, reducing tissue inflammation, improving barrier function, and regulating gut flora. These results highlight that it may be a promising probiotic for alleviating HUA.

Keywords: *Lactiplantibacillus plantarum* CCNH185; Hyperuricemia; uric acid; Nucleoside degradation; intestinal barrier; gut microbiota

Check for updates

Academic Editor: Mauro Rossi

Received: 3 October 2026
Revised: 13 November 2026
Accepted: 21 November 2026
Published: 26 November 2026

Copyright: © 2026 by the authors. Licensee MDPI, Basel, Switzerland. This article is an open access article distributed under the terms and conditions of the Creative Commons Attribution (CC BY) license.

1. Introduction

Hyperuricemia (HUA) manifests as a metabolic condition triggered by impaired purine processing, which leads to an increase in serum uric acid (UA) levels [1,2]. If circulating UA concentrations exceed 0.42 mmol/L (7 mg/dL), a diagnosis of HUA can be established [3]. Among Chinese adults, the HUA prevalence experienced a notable rise, climbing from 11.1% during 2015–2016 to 14% by 2018–2019 [4]. The occurrence of HUA is closely associated with multiple factors, including genetic background, sex differences, lifestyle, and dietary habits [5]. When the concentration of UA is too high, it will cause inflammation in the body [6,7]. Long-term HUA often causes UA crystals to deposit in joints and induce gout. At

the same time, it is associated with an increased risk of cardiovascular disease, hypertension, type 2 diabetes and chronic kidney disease, although whether these associations are causal remains to be fully established. HUA seriously affects people's quality of life, so identifying safe dietary adjunct strategies is of public health and clinical relevance.

UA is predominantly produced within the hepatic tissue; consequently, crucial enzymes in this organ are essential for its biosynthesis. Adenosine monophosphate is deaminated and dephosphorylated into inosine, and guanine monophosphate is directly converted into guanosine by nucleotide enzymes. Via the catalytic action of purine nucleoside phosphorylase (PNP), inosine undergoes further conversion to hypoxanthine, and guanosine is transformed into guanine. Both hypoxanthine and guanine yield xanthine; the former is oxidatively processed by xanthine oxidase (XOD), whereas the latter is directly deaminated. Finally, xanthine is subsequently processed into UA through XOD catalysis [8]. Excessive XOD activity increases UA production and contributes to the development. Their excessive activation will lead to increased UA production, which in turn promotes the occurrence of HUA. Endogenous UA is primarily eliminated through the renal and intestinal tracts, accounting for approximately 70% and 30%, respectively [9,10]. UA transporters are essential for UA elimination, predominantly localizing to the basolateral and/or apical membranes of both proximal renal tubules and intestinal epithelial cells [11]. At present, the main treatment methods for HUA are diet control and drug treatment, including allopurinol [12], febuxostat [13] and benzbromarone [14]. However, prolonged administration frequently induces adverse reactions, including hepatotoxicity as well as renal hypersensitivity [15]. These therapies might individually provoke adverse reactions, including allopurinol hypersensitivity, liver enzyme elevation and hepatotoxicity, respectively, and long-term use requires appropriate monitoring.

Evidence indicates that probiotics exert a mitigating effect on HUA via complementary mechanisms, including the degradation of nucleosides by bacterial hydrolases, inhibition of hepatic UA synthesis, modulation of UA transporters in the kidney and intestine, improving the gut barrier function, as well as modulating the gut flora. These findings suggest that probiotics may act at multiple sites along the purine metabolic pathway, although the relative contribution of each mechanism remains strain-dependent and incompletely defined. *Lacticaseibacillus rhamnosus* CCFM1130, *Limosilactobacillus reuteri* CCFM1132 and *Lacticaseibacillus rhamnosus* CCFM1131 can boost intestinal SCFAs synthesis and further inhibit XOD activity to alleviate HUA [16]. *Lactiplantibacillus plantarum* has three intracellular nucleoside hydrolases, RihA, RihB and RihC, which achieve efficient hydrolysis of nucleosides by synergistic catalysis and eventually generate nucleobases, thereby alleviating HUA by reducing substrates for UA synthesis [17]. *Lactococcus cremoris* D2022 can up-regulate OAT1/2/3 and ABCG2, while inhibiting GLUT9 and URAT1 to lower blood UA levels [18]. *Lacticaseibacillus rhamnosus* Fmb14 can elevate ZO-1 and occludin transcript levels, thereby reducing the entry of UA and inflammatory factors from the intestinal cavity into the blood [19]. In addition, probiotics are capable of restoring gut microbial homeostasis while fortifying the HUA-injured gut barrier. Previous research indicates that probiotics are capable of mitigating HUA by modulating gut microbiota-derived tryptophan metabolism, restoring intestinal barrier integrity, and promoting colonic UA excretion [20].

It remains unclear whether a single *L. plantarum* strain with superior simultaneous degradation of both inosine and guanosine can coordinately modulate hepatic UA production, UA transport across the kidney and intestine, gut barrier function, inflammation and gut microbiota during HUA. *L. plantarum* CCNH185 can regulate innate immunity and inhibit inflammatory response [21]. This study aimed to identify probiotics capable of degrading inosine and guanosine in vitro using high-performance liquid chromatography (HPLC), while HUA mice induced through oral administration of potassium oxonate,

inosine, and guanosine were used as the model to evaluate its UA-lowering effect. We hypothesized that CCNH185 would alleviate HUA by reducing UA precursors and coordinately regulating hepatic UA synthesis, renal and intestinal urate transport, intestinal barrier function and gut microbiota composition. To test this hypothesis, we (i) evaluated the UA-reducing efficacy of CCNH185 within a purine-induced HUA mouse model; (ii) measured hepatic XOD, PNP and ADA activity and mRNA expression; (iii) examined the expression of UA transporters across the kidney and intestine, as well as intestinal barrier-associated proteins; (iv) assessed inflammatory cytokine mRNA expression in the colon and liver; and (v) integrated targeted serum metabolomics and metagenomic microbiota analysis to characterize the systemic and microbial responses to CCNH185 intervention. This work provides a wealth of evidence to determine the precise function of CCNH185 in reducing serum UA to alleviate HUA.

2. Materials and Methods

2.1. Microbial Strains and Cultivation Parameters

Fifteen *L. plantarum* isolates obtained from fermented foods and human fecal samples were revived from glycerol stocks (−80 °C) via streaking on de Man, Rogosa and Sharpe (MRS) agar. Following a 24 h incubation at 37 °C, distinct individual colonies were picked and transferred into liquid MRS broth, which was cultured for another 24 h at 37 °C. Thereafter, a 2% (*v*/*v*) inoculum was transferred into fresh MRS broth (Aoboxing Biotech, Beijing, China) and cultivated at 37 °C for 12 h.

2.2. Determination of Nucleoside Degradation Ability in Vitro

We measured the in vitro capacity of the strains to degrade nucleosides based on an adapted procedure [22]. After subculturing for three generations, pellets from 1 mL of culture broth were collected by centrifugation (6000× *g*, 5 min, 4 °C). Subsequently, the resulting pellets were rinsed thrice using sterile phosphate-buffered saline (PBS, pH 7.2) and re-dispersed in a 0.5 g/L standard solution (1 mL total) containing inosine and guanosine. Following a 1-h incubation at 37 °C, the reaction mixture was spun down (8000× *g*, 4 °C, 5 min) to harvest the supernatant. To quench the reaction, 0.1 mol/L $HClO_4$ (9:1, *v*/*v*) was mixed with the supernatant. Subsequently, following filtration using a membrane (0.22 μm), a 10-microliter aliquot was loaded onto the Shimadzu LC-20A HPLC (Kyoto, Japan) to quantify residual nucleoside in the reaction solution. PBS functioned as a blank control against background noise. Separation was achieved on an INERTSUSTAIN AX-C18 column (5 μm, 4.6 × 250 mm). A gradient mobile phase of 10 mM KH_2PO_4 and methanol (95:5, *v*/*v*) was applied at 1 mL/min. The column was kept at 30 °C, with UV detection at 254 nm and a total run time of 15 min. Nucleoside levels were quantified using an HPLC system with the external standard method.

$$\text{Nucleoside degradation rate } (\%) = (C_{\text{mother liquor}} - 10/9C_{\text{residue}})/C_{\text{mother liquor}}$$

2.3. Preparation of Bacterial Suspension for Animal Experiment

The viable count of *L. plantarum* CCNH185 in the stable phase was determined by plate counting method, and the corresponding OD value was determined by ultraviolet spectrophotometer. Subsequently, 2% (*v*/*v*) inoculum was transferred into liquid MRS, followed by a 12 h incubation at 37 °C. The harvested pellets were washed 2–3 times with sterile PBS and finally reconstituted using PBS. The viable bacterial density was then standardized to 1×10^{10} CFU/mL to prepare the inoculum for oral gavage during the experimental period.

2.4. Animal Procedures

Male Kunming mice (SPF grade, 3 weeks old, 18–21 g) were obtained from Beijing Vital River Laboratory Animal Technology (Beijing, China). The Animal Ethics Committee of China Agricultural University approved all animal procedures in this study (Approval Number. Aw52905202-5-2). Prior to the experiments, the mice underwent a one-week acclimation in standard housing facilities. Environmental settings were strictly regulated at 23 ± 1 °C, 55 ± 15% humidity, and a 12-h photoperiod (light/dark). All mice were randomized to three cohorts (n = 6): a control (CK), a HUA model (MOD), and an *L. plantarum* CCNH185-treated arm (CCNH185). Mice in all cohorts had free access to standard laboratory chow provided by Sipeifu Biotechnology (Beijing, China) and water. To induce HUA, mice received an oral gavage of 250 mg/kg potassium oxonate, 400 mg/kg inosine (Rhawn, Shanghai, China), and 400 mg/kg guanosine (Rhawn, Shanghai, China), prepared in 0.5% (w/v) carboxymethylcellulose sodium. The control mice received an isovolumetric dose of 0.5% (w/v) carboxymethylcellulose sodium and 1× PBS via oral gavage. The CCNH185 group was intragastrically administered the HUA-inducing mixture together with 1×10^9 CFU/d bacterial suspension for 21 days. Following overnight fasting, mice were euthanized via cervical dislocation. Blood, along with liver, kidney, intestinal tissues, and fecal material, was collected. These specimens were rapidly frozen and subsequently preserved at −80 °C.

2.5. Measuring Serum Metabolic Indicators

We allowed the gathered blood to settle at ambient temperature for 120 min. Following centrifugation at 3500 r/min for 15 min at 4 °C, we obtained serum and stored it at −80 °C. We measured serum UA, blood urea nitrogen (BUN), and creatinine (CR) using commercial kits (Jiancheng, Nanjing, China), following the provided directions.

2.6. Histopathologic Analysis

Following 24 h fixation in 4% paraformaldehyde, the intestine, kidney and liver underwent paraffin embedding. Using a Servicebio PM-24 microtome (Servicebio, Wuhan, China), 5-micrometer-thick tissue slices were obtained from each embedded block. The slices were deparaffinized in xylene, rehydrated through a graded ethanol series of 100%, 95%, 85% and 75%, and then stained with hematoxylin–eosin.

2.7. Liver Xod, Pnp and Ada Activity Measurement

Upon completing the homogenization of liver specimens under ice-bath conditions, we subjected samples to centrifugation (10,000× g, 10 min, 4 °C), and the resulting clarified liquid was harvested for downstream biochemical assays. Assessments of XOD, adenosine deaminase (ADA), and PNP activities were carried out based on the accompanying kit protocols of XOD (Solarbio, BC1095, Beijing, China), ADA (Solarbio, BC6325, Beijing, China) and PNP (Solarbio, BC6350, Beijing, China) assay kits.

2.8. Quantitative Reverse Transcription PCR

Isolation of total RNA from murine kidney, liver and intestine samples was performed by means of AG RNAex Pro reagent (Accurate Biotechnology, Changsha, China), based on official kit guidelines. For cDNA generation, we implemented the two-step reaction procedure described in the Evo M-MLV RT Premix kit (Accurate Biotechnology, Changsha, China). The SYBR Green Premix Pro Taq Hs qPCR kit (Accurate Biotechnology, Changsha, China) was utilized to carry out RT-qPCR assays on the QuantStudio™7 instrument (Applied Biosystems, Thermo Fisher Scientific Inc., Waltham, MA, USA). Detailed sequences

for the utilized primers can be found in Table 1. The reference genes and primer sequences were selected by Jing et al. [23].

Table 1. qRT-PCR primers used in this work.

Gene	Forward Primer (5′–3′)	Reverse Primer (5′–3′)
β-Actin	GTGACGTTGACATCCGTAAAGA	GCCGGACTCATCGTACTCC
Glut9	TTGCTTTAGCTTCCCTGATGTG	GAGAGGTTGTACCCGTAGAGG
Oat1	CTGATGGCTTCCCACAACAC	GTCCTTGCTTGTCCAGGGG
Urat1	TCACCACCCAGAACATGCTG	GGAGACGGCCAGAAGAACAT
Abcg2	GAACTCCAGAGCCGTTAGGAC	CAGAATAGCATTAAGGCCAGGTT
Xod	ATGACGAGGACAACGGTAGAT	TCATACTTGGAGATCATCACGGT
Pnp	CAACACACTGAATATCGACCTCA	GCTTTGGGGAAAGTTGGGTATCT
Ada	ACCCGCATTCAACAAACCCA	AGGGCGATGCCTCTCTTCT
Oat3	ATGACCTTCTCCGAGATTCTGG	GTGGTTGGCTATTCCGAGGAT
Npt1	TCTGTTCCTTCCGGTATGGAC	AGAACTGAGAATAAGCCCTTGGA
ZO-1	GCCGCTAAGAGCACAGCAA	TCCCCACTCTGAAAATGAGGA
Muc2	TGCTGACGAGTGGTTGGTGAAT	GATGAGGTGGCAGACAGGAGAC
Claudin-1	GGGGACAACATCGTGACCG	AGGAGTCGAAGACTTTGCACT
Claudin-15	ATGTCGGTAGCTGTGGAGAC	GGACGGAAAGTCCCAGCAG
Il-1β	GCAACTGTTCCTGAACTCAACT	ATCTTTTGGGGTCCGTCAACT
Il-6	TAGTCCTTCCTACCCCAATTTCC	TTGGTCCTTAGCCACTCCTTC
Il-10	GCTCTTACTGACTGGCATGAG	CGCAGCTCTAGGAGCATGTG
Tnf-α	CCCTCACACTCAGATCATCTTCT	GCTACGACGTGGGCTACAG

2.9. Immunofluorescence Staining

Xylene and gradient ethanol were applied for dewaxing and rehydration of kidney and colon sections. Subsequently, antigen retrieval was carried out with citrate buffer (pH 6.0). At ambient temperature, sections were incubated in 1% Triton X-100 for permeabilization and then incubated in immunostaining blocking solution (Beyotime, Shanghai, China) for 60 min. The primary antibodies targeting GLUT9 (Proteintech, 26486-1-AP, 1:500) and ABCG2 (Santa Cruz Biotechnology, sc-58222, 1:500) were applied for overnight incubation at 4 °C. Following washes, Sections were exposed to Alexa Fluor 488-conjugated secondary antibody (Abcam, ab150077, 1:1000) for 60 min at ambient temperature in darkness. Finally, DAPI (Beyotime, Shanghai, China) was applied for nuclear counterstaining, followed by coverslip placement with anti-fade mounting reagent. The Zeiss Axio Imager M.2 fluorescence microscope (Carl Zeiss AG, Oberkochen, Germany) was utilized to record images, and protein expression was quantified using ImageJ software (version 1.54r).

2.10. Analysis of Serum Targeted Metabolites

Following thawing in an ice-water bath, the serum was mixed thoroughly. Next, 100 µL of serum was taken and four times the volume of internal standard-supplemented methanol was added to fully mix. Following 15 min of sonication in a bath of ice and water, the mixture was placed at −40 °C for 60 min. After centrifugation (4 °C, 13,800× *g*, 15 min), 200 µL of supernatant was taken into a vial for liquid chromatography-tandem mass spectrometry detection. The same quantities of supernatant from all samples were mixed as a quality control sample. A series of dilutions of the mixed standard solution was used to prepare the calibration curve. Liquid chromatography separation was performed on a UPLC system equipped with an ACQUITY UPLC BEH C18 column (Agilent 1290 UPLC). HILIC separation was performed on an Agilent 1290 Infinity II UHPLC system fitted with an Atlantis Premier BEH Z-HILIC column. Mass spectrometric analysis was performed on a Sciex Triple Quad 6500+ (ESI source) in MRM mode, with a curtain gas of 35 psi, ion spray voltages of +5000/−4500 V, a temperature of 400 °C, and ion source gases

1 and 2 both at 50 psi. Data acquisition and quantitative analysis were performed using Analyst 1.7.32 and BioBud v2.0.4.

2.11. Metagenomic Analysis of Gut Microbiota

Stool samples were processed for DNA extraction employing the magnetic bead-based FastPure Stool DNA Isolation Kit (MJYH, Shanghai, China). The yield and purity of the isolated DNA were quantified using a Synergy HTX microplate reader and a NanoDrop 2000 spectrophotometer. DNA integrity was further checked by agarose gel electrophoresis. DNA was fragmented to an average length of approximately 350 bp using a Covaris M220 focused-ultrasonicator. A paired-end sequencing library was then constructed with the NEXTFLEX Rapid DNA-Seq Kit (Bioo Scientific, Austin, TX, USA). Data quality control (QC) and filtering: To ensure sufficient sequencing depth for metagenomic coverage, raw sequencing reads were strictly processed using the standard Majorbio Cloud pipeline. Low-quality sequences (including those with adapter contamination, ambiguous bases, or low-quality scores) and host-derived reads were filtered out to obtain clean data for downstream analysis, ensuring the reliability of the results. The Majorbio Cloud platform (https://cloud.majorbio.com) was used for all bioinformatics analyses.

2.12. Statistical Analysis

GraphPad Prism 10.4.2 statistical analysis software was used to process the experimental data, and the results were expressed as mean ± SEM. Species-level differential abundance in metagenomic data was assessed by the Wilcoxon rank-sum test, and associations between bacterial genera and biochemical parameters were assessed by Spearman correlation analysis. Other data were analyzed using one-way ANOVA and Tukey's post hoc multiple comparison test was used to analyze the differences between groups. For Figure 1, different lowercase letters above the bars indicate significant differences among strains ($p < 0.05$), and bars sharing the same letter are not significantly different. A two-tailed $\alpha = 0.05$ was set as the significance threshold. $p < 0.05$ was considered statistically significant.

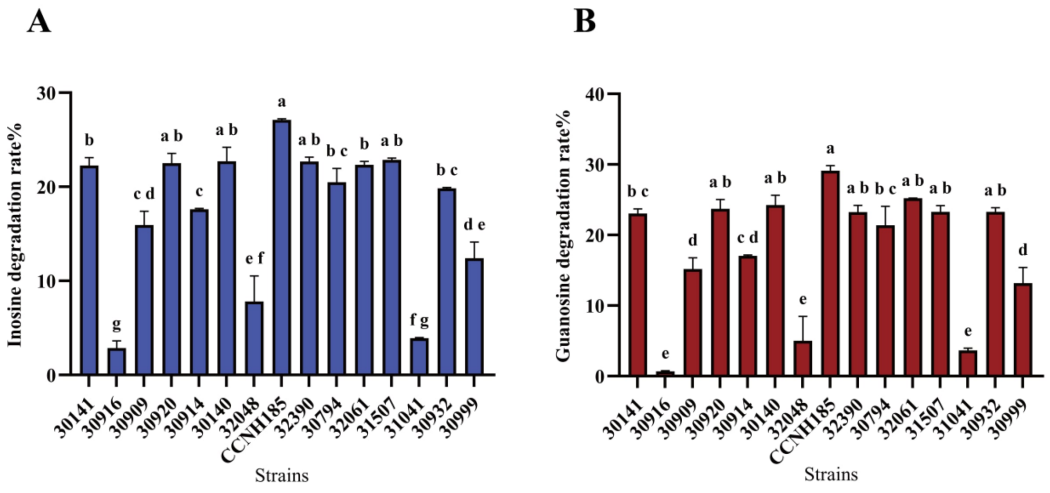

Figure 1. Nucleoside degradation ability of 15 strains of *L. plantarum* in vitro. (**A**) Inosine degradation rate. (**B**) Guanosine degradation rate. All data are presented as the mean ± S.E.M. $n = 3$. In each subgraph, the different letters above the bar indicate significant differences between groups ($p < 0.05$). Bars with the same letter are not significantly different.

3. Results

3.1. In Vitro Screening of L. plantarum Strains with Ua-Lowering Activity

To obtain a *L. plantarum* strain with the effective ability to degrade nucleosides, 15 strains were analyzed using high-performance liquid chromatography. Among them, *L. plantarum* CCNH185 has the strongest in vitro degradation ability for inosine and guanosine; the degradation rate reached 27.12% (Figure 1A) and 29.10% (Figure 1B), respectively. Therefore, we selected *L. plantarum* CCNH185 to further explore its ability to reduce UA in vivo.

3.2. L. plantarum Ccnh185 Ameliorates Purine-Induced HUA in Mice

The mouse model of elevated UA was established to assess the impact of *L. plantarum* CCNH185 on HUA (Figure 2A). Body weight was recorded every 7 days throughout the 21-day experiment. At the end of the 21-day intervention, no significant intergroup difference in body weight was observed (Figure 2B). After three weeks of treatment, serum UA levels in the model group were nearly 1.4-fold those of the control group, and administration of *L. plantarum* CCNH185 markedly alleviated HUA (Figure 2C).

Serum creatinine (Scr) and blood urea nitrogen (BUN) were markedly elevated in the MOD group relative to the CK group, suggesting impaired renal function and reduced excretory capacity. In contrast, the CCNH185 group significantly down-regulated Scr and BUN levels (Figure 2D,E). Histopathological examination revealed epithelial cell shedding, mucosal discontinuity, reduced goblet cells, and marked inflammatory cell infiltration in the colon of MOD group mice. In addition, kidney injury was additionally detected, manifested as abnormal glomerular volume, narrowed glomerular cystic space, and capillary loop dilatation and mild renal interstitial congestion. The CCNH185 group had a significant effect in alleviating intestinal and renal injury. The liver sections of mice in the MOD group showed disordered hepatic lobule structure, loose arrangement of hepatocytes, vacuolization of cytoplasm, and significant inflammatory cell infiltration. By contrast, CCNH185 treatment significantly reduced liver pathological damage (Figure 2F).

Subsequently, inflammatory cytokine expression in the colon and liver was measured. The results showed that the colonic pro-inflammatory factor MOD group exhibited a significant increase in *IL-1β* ($p < 0.05$) and a significant decrease in anti-inflammatory *IL-10* ($p < 0.01$) relative to the CK group (Figure 2G,H). Additionally, hepatic expression of pro-inflammatory cytokines was significantly higher in the MOD group than in the CK group ($p < 0.05$), including *IL-1β* ($p < 0.001$) and *IL-6* ($p < 0.01$), while the anti-inflammatory cytokine *IL-10* was significantly reduced (Figure 2I–L). In contrast, colonic and hepatic inflammatory cytokine levels in the colon and liver of the CCNH185 group returned to normal. These findings reveal that *L. plantarum* CCNH185 has a significant ameliorative effect on the symptoms of HUA.

3.3. L. plantarum Ccnh185 Inhibits the Activity of Ua Synthesis-Related Enzymes in the Liver

Overactivation of hepatic UA-synthesizing enzymes such as XOD, PNP, and ADA can elevate UA production and accelerate HUA development. After 3 weeks of intervention, the MOD group exhibited significantly higher hepatic XOD, PNP, and ADA activities than the CK group (Figure 3A–C). At the same time, the hepatic mRNA expression of *XOD*, *PNP*, and *ADA* was also significantly up-regulated (Figure 3D–F), whereas probiotic treatment significantly reduced the activities and transcriptional levels of XOD, ADA, and PNP in the liver. The present results suggest that the UA-lowering effect of *L. plantarum* CCNH185 may be associated with its inhibition of hepatic UA synthesis-related enzyme activities.

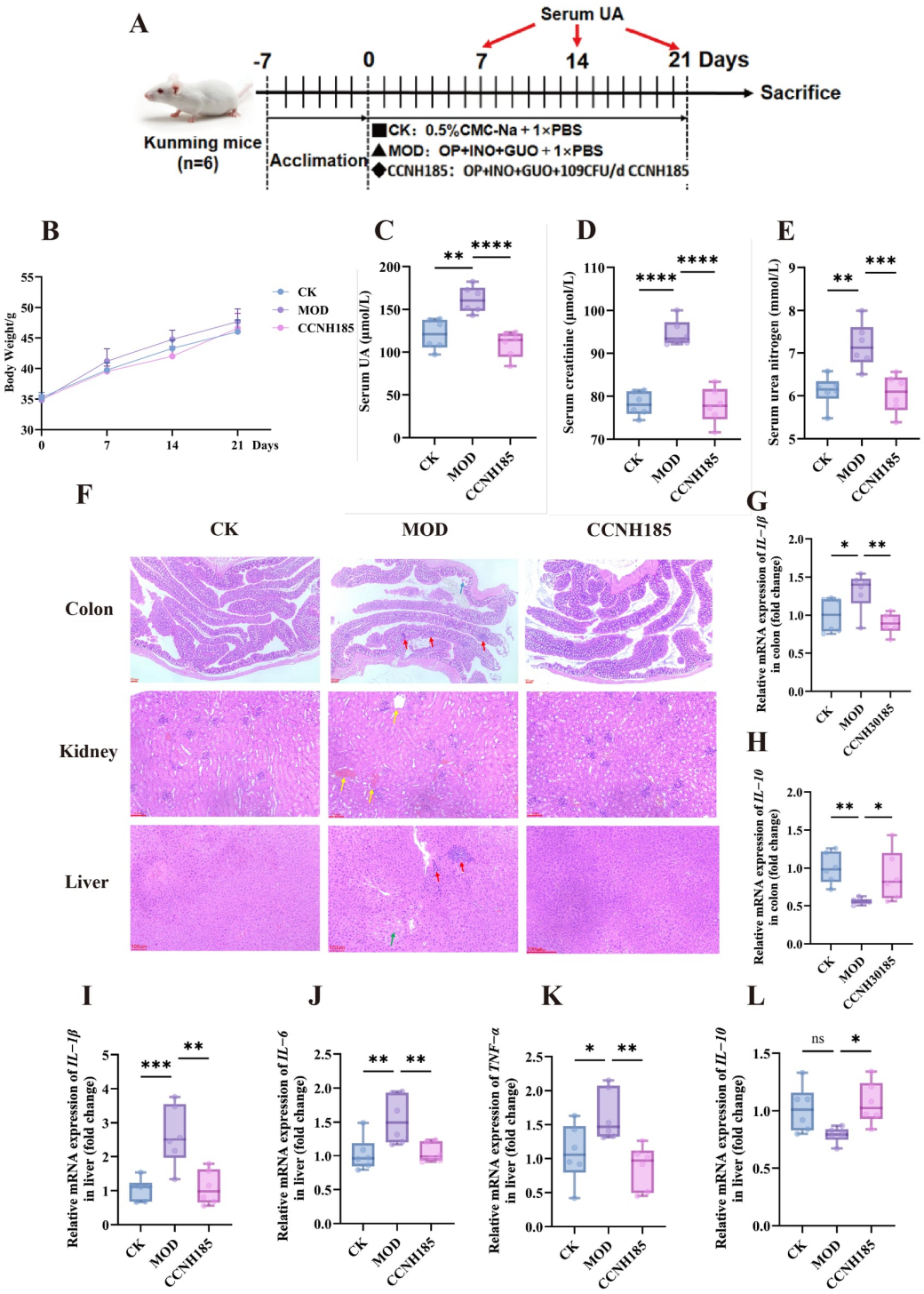

Figure 2. Effect of *L. plantarum* CCNH185 on hyperuricemia symptoms. (**A**) Flow chart of animal treatment experiment. (**B**) Body weight. (**C**) Serum UA. (**D**) Scr. (**E**) BUN. (**F**) Representative H & E staining images of tissue sections. The red arrows represent inflammatory cell infiltration, the blue arrow represents epithelial cell shedding, the yellow arrows represent interstitial congestion and capillary loop dilatation, and the green arrow represents cytoplasmic vacuolization. $n = 3$ mice per group. (**G**–**J**) mRNA levels of inflammatory cytokines in the liver tissues for each group. (**G**) *IL-1β* and (**H**) *IL-10* in the colon, and (**I**) *IL-1β*, (**J**) *IL-6*, (**K**) *TNF-α* and (**L**) *IL-10* in the liver: mRNA levels of inflammatory cytokines for each group. $n = 6$ mice per group. All data are presented as the mean ± S.E.M. * $p < 0.05$, ** $p < 0.01$, *** $p < 0.001$, **** $p < 0.0001$, ns, not significantly.

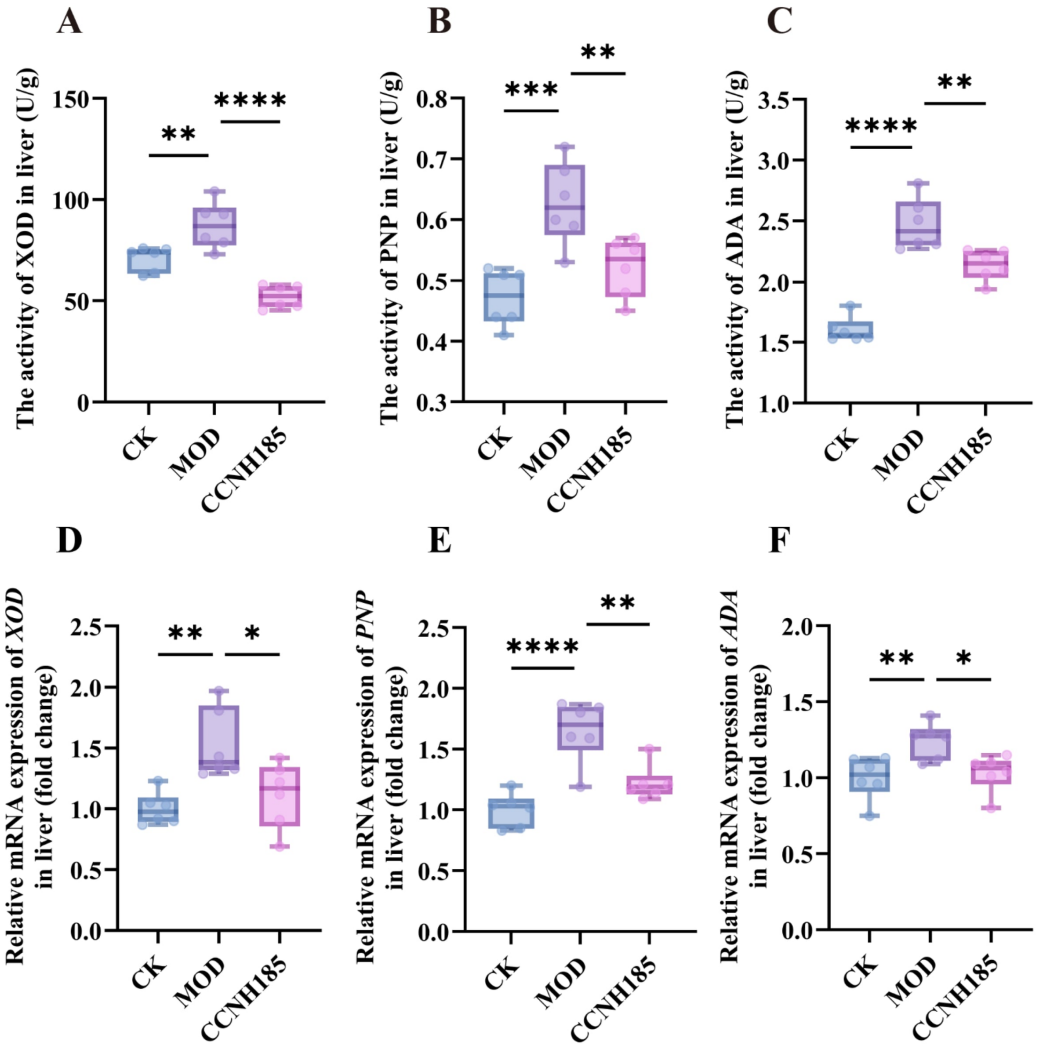

Figure 3. Effect of *L. plantarum* CCNH185 on UA synthesis and antioxidant activity. Enzymatic activities of XOD (**A**), PNP (**B**) and ADA (**C**) in liver. mRNA levels of XOD (**D**), PNP (**E**) and ADA (**F**) in liver. $n = 6$ mice per group. All data are presented as the mean ± S.E.M. * $p < 0.05$, ** $p < 0.01$, *** $p < 0.001$, **** $p < 0.0001$.

3.4. L. plantarum Ccnh185 Regulates Ua Levels by Regulating Renal Ua Transporters in HUA Mice

UA transporters are critical for UA homeostasis. They are mainly classified into reabsorption transporters, including GLUT9 and URAT1, and excretion transporters, including ABCG2, OAT1, OAT3, and NPT1. In this study, relative to the CK group, the MOD group showed significantly elevated expression of *URAT1* and *GLUT9*, but significantly reduced expression of *ABCG2*, *OAT1*, *OAT3*, and *NPT1*. However, *L. plantarum* CCNH185 significantly inhibited URAT1 and GLUT9 expression by 34.4% and 26.0%, respectively (Figure 4A,B), and significantly promoted the expression of *OAT1*, *OAT3*, *ABCG2* and *NPT1* by 70.9%, 117.8%, 50.0% and 49.2%, respectively (Figure 4C–F). To further verify the relative expression levels of GLUT9 and ABCG2, immunofluorescence analysis of mouse kidneys was performed. GLUT9 protein expression was significantly decreased and ABCG2 protein expression was significantly increased in the CCNH185 group relative to the MOD group (Figure 4G–J). The findings showed that *L. plantarum* CCNH185 could alleviate HUA by regulating the expression level of UA transporters.

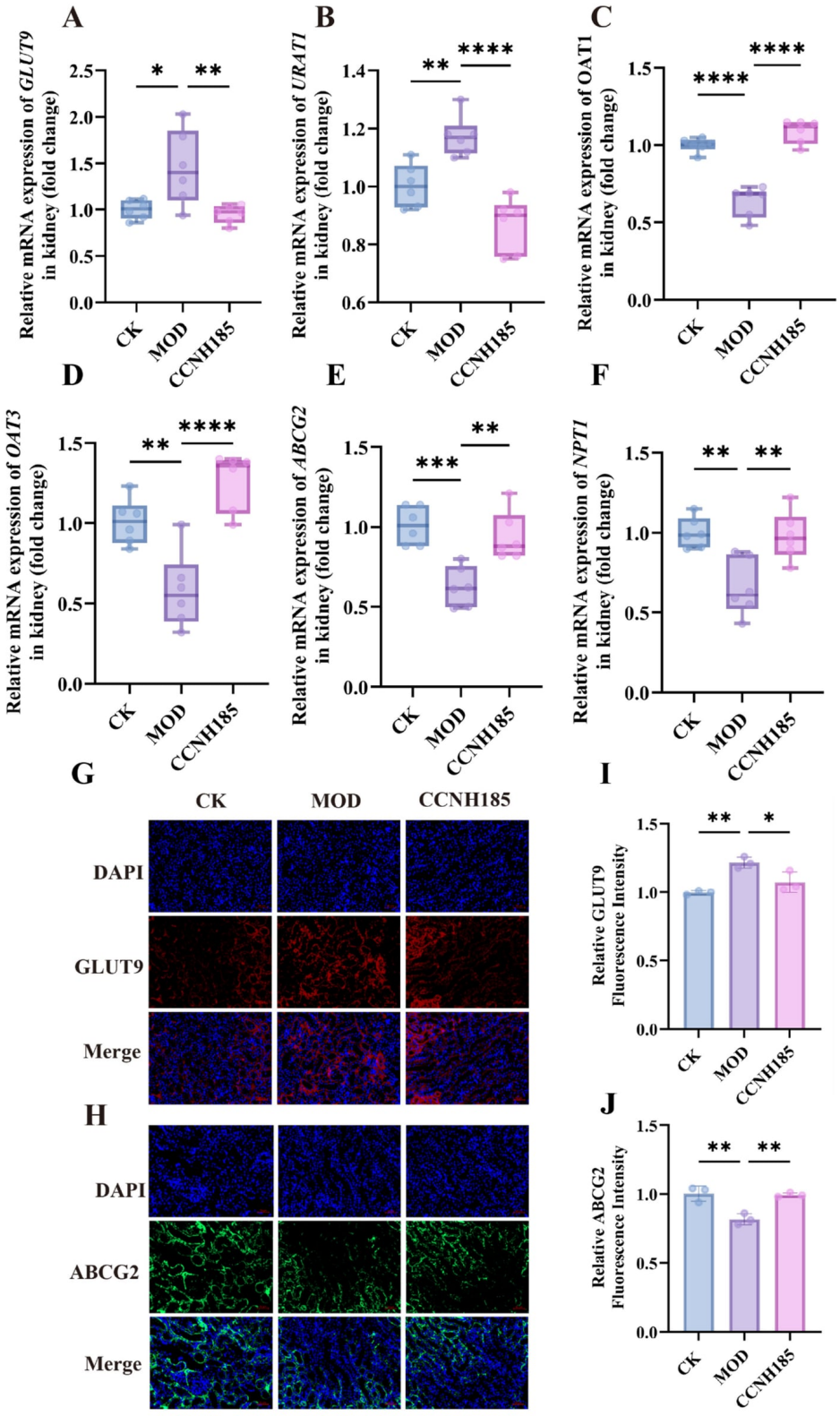

Figure 4. Effects of *L. plantarum* CCNH185 on renal UA transporters. The mRNA expression levels of (**A**) *GLUT9*, (**B**) *URAT1*, (**C**) *OAT1* and (**D**) *OAT3*, (**E**) *ABCG2* and (**F**) *NPT1* in the kidney. $n = 6$ mice per group. Representative immunofluorescence staining images of (**G**) GLUT9 (red) and (**H**) ABCG2 (green). Nuclei were stained by DAPI (blue). Scale bar means 50 μm. Quantification of (**I**) GLUT9 and (**J**) ABCG2 fluorescence intensity. $n = 3$ mice per group. All data are presented as the mean ± S.E.M. * $p < 0.05$, ** $p < 0.01$, *** $p < 0.001$, **** $p < 0.0001$.

3.5. L. plantarum CCNH185 Improves HUA by Regulating Intestinal UA Transporters and Repairing Intestinal Barrier Damage

In intestinal tissue, the expression level of the *ABCG2* gene in ileum tissue of the MOD group was significantly down-regulated by 34.7%, while the expression level of *GLUT9* in colon was significantly up-regulated by 68.7% (Figure 5A,B). *L. plantarum* CCNH185 intervention significantly up-regulated the expression level of *ABCG2* in ileum tissue ($p < 0.05$), and significantly down-regulated the expression level of *GLUT9* in colon ($p < 0.05$). HUA is associated with intestinal barrier damage, and the expression of intestinal barrier proteins was further measured to evaluate the ability of *L. plantarum* CCNH185 to repair barrier damage. The expression levels of *ZO-1*, *Muc2*, *Claudin-1*, and *Claudin-15* in colonic tissue were significantly decreased in the MOD group relative to the CK group, with decreases of 27.1%, 46.2%, 37.0%, and 25.1%, respectively. (Figure 5C–F). After *L. plantarum* CCNH185 intervention, the expression levels of *ZO-1*, *Muc2*, *Claudin-1* and *Claudin-15* were significantly increased by 26.1%, 57.6%, 58.45% and 55.2%, respectively. Immunofluorescence analysis further confirmed that colonic GLUT9 protein expression in the CCNH185 group was significantly lower than that in the MOD group (Figure 5G,H). The results showed that *L. plantarum* CCNH185 may alleviate HUA by reducing UA reabsorption and increasing excretion, and repairing colonic barrier damage.

3.6. Determination of Serum Metabolites in Mice

To explore the effective mechanism of *L. plantarun* CCNH185 to alleviate HUA, the changes in metabolites in serum were analyzed using AQ500 targeted metabolomics technology. A total of 15 categories and 313 metabolites, such as nucleosides, purines, pyrimidines and organic acids, were identified by mass spectrometry and spectral comparison. The results of PCA analysis showed that serum metabolites were significantly deviated after *L. plantarum* CCNH185 intervention from those of the CK and MOD groups (Figure 6A). Differential metabolite analysis revealed that the concentrations of 18 metabolites were significantly higher in the MOD group than in the CK group, whereas the concentrations of 10 metabolites were significantly lower (Figure 6B). Relative to the MOD group, the CCNH185 group exhibited significantly higher concentrations of 18 metabolites and significantly lower concentrations of 44 metabolites (Figure 6C). As shown in Figure 6D, relative to the CK group, UA content was significantly elevated in the MOD group; this increase was significantly attenuated by *L. plantarum* CCNH185 intervention.

Further, the key metabolites in serum after *L. plantarum* CCNH185 intervention were quantitatively analyzed. After intervention with *L. plantarum* CCNH185, the serum levels of UA, inosine, and xanthosine returned to levels comparable to those in the CK group (Figure 6E–G). Inosine and xanthosine are important precursors of UA synthesis, and the reduction of these precursors is conducive to reducing the synthesis of UA in the liver. Compared with the CK group and the MOD group, *L. plantarum* CCNH185 intervention could increase the content of organic acids in serum, especially the content of salicylic acid, which reached an average of 276.2 nmol/L, an increase of 5.7 times (Figure 6H). Salicylic acid has anti-inflammatory function [24], and the increase in its level may indicate that the body's inflammatory state has been alleviated. On the one hand, salicylic acid can reduce prostaglandin synthesis by inhibiting the cyclooxygenase pathway, thereby inhibiting the inflammatory response [25]; on the other hand, it can also suppress the production of oxygen-derived free radicals by xanthine oxidase; through this reduction in oxidative stress, it may indirectly limit xanthine oxidase-driven UA production [26]. Serum prostaglandin E2 was indeed significantly increased in the MOD group, while prostaglandin E2 was not detected in the *L. plantarum* CCNH185 intervention group (Figure 6I), indicating that systemic inflammation was alleviated after intervention. In addition, serum reduced

glutathione (GSH) levels increased to 1028 nmol/L after *L. plantarum* CCNH185 intervention, representing a 2.2-fold increase (Figure 6J). As one of the most important endogenous antioxidant molecules in the body, GSH can scavenge ROS and maintain cellular redox homeostasis. Xanthine oxidase activity and oxidative stress are mechanistically coupled: XOD-catalyzed UA production generates superoxide and hydrogen peroxide, and this oxidative burden is associated with further amplification of purine catabolism and UA production [27]. Therefore, the increase of GSH level helps to alleviate oxidative stress and may thereby indirectly inhibiting the excessive production of UA. These results showed that *L. plantarum* CCNH185 intervention not only may inhibit UA production in vivo, but also have anti-inflammatory and anti-oxidative damage effects.

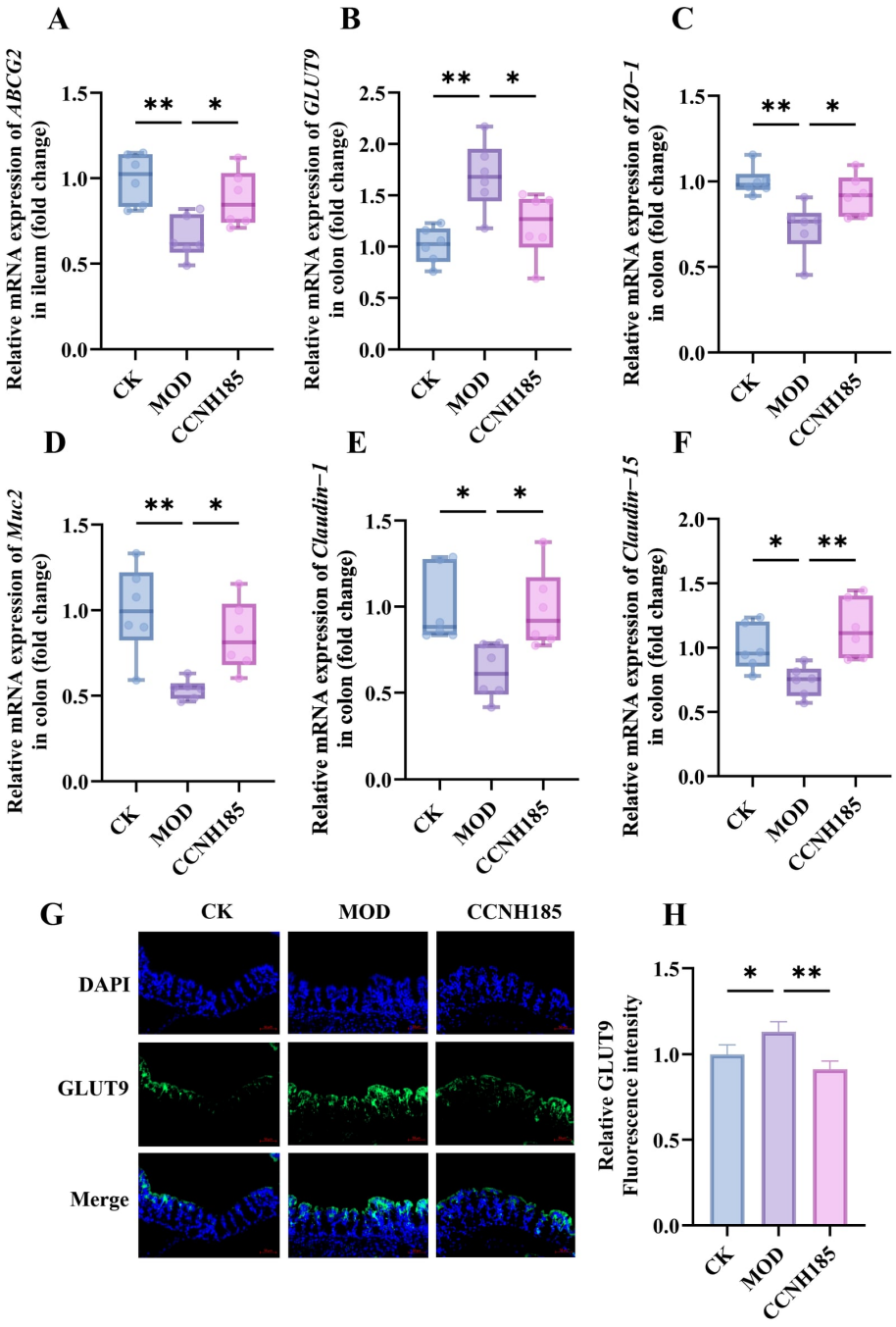

Figure 5. Effects of *L. plantarum* CCNH185 on intestinal UA transporter and intestinal barrier in hyperuricemic mice. The mRNA expression levels of (**A**) *ABCG2* in ileum and (**B**) *GLUT9*, (**C**) *ZO-1*,

(**D**) *Muc2*, (**E**) *Claudin-1* and (**F**) *Claudin-15* in the colon. $n = 6$ mice per group. (**G**) Representative immunofluorescence staining images of ABCG2 (green). Nuclei were stained with DAPI (blue). Scale bar means 50 μm. (**H**) Quantification of GLUT9 fluorescence intensity. $n = 3$ mice per group. All data are presented as the mean ± S.E.M. ($n = 6$). * $p < 0.05$, ** $p < 0.01$.

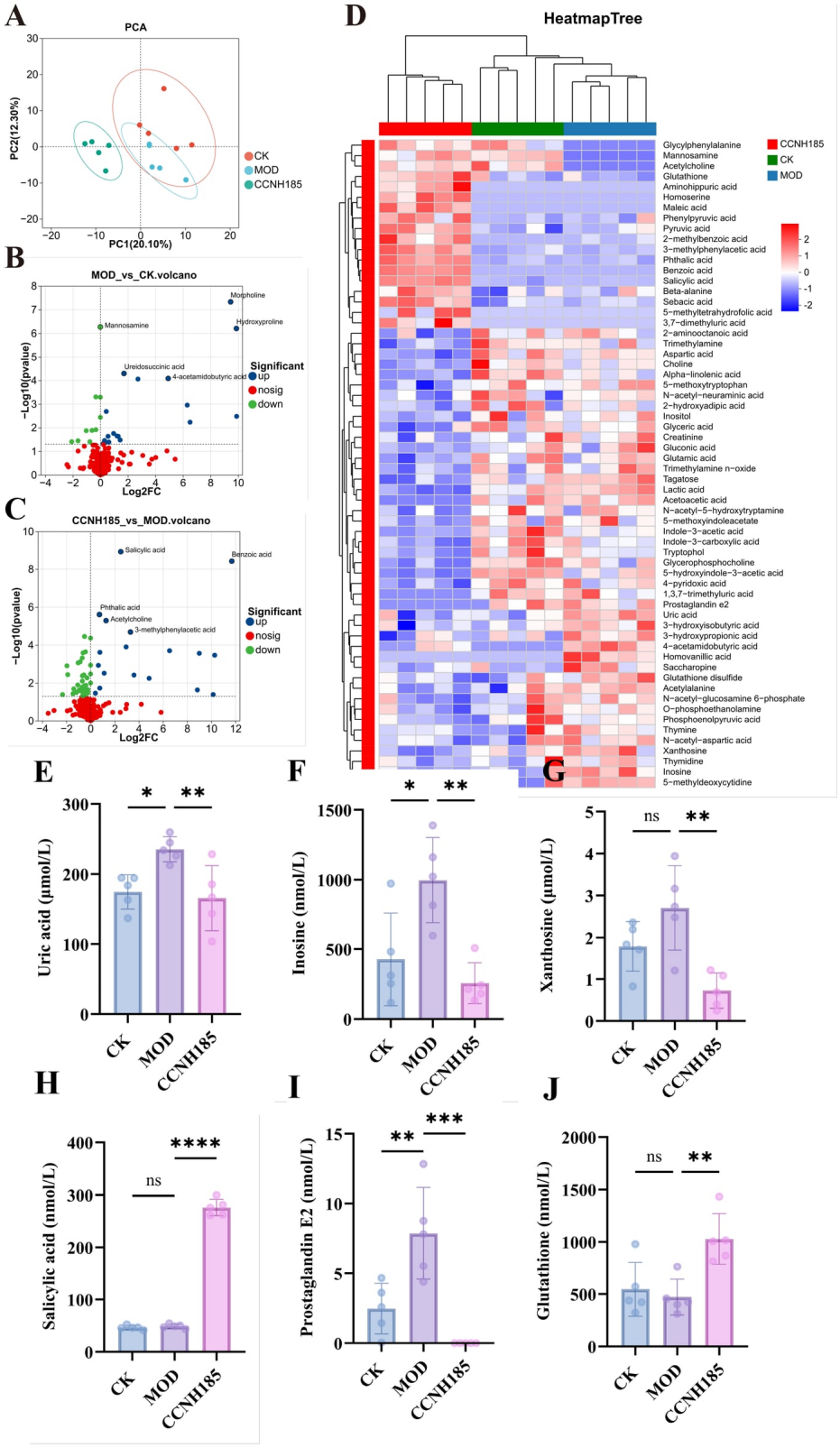

Figure 6. The composition of serum metabolites changed significantly. (**A**) Principal component analysis (PCA). (**B**) Differential metabolites volcano plot (MOD vs. CK). (**C**) Differential metabolites

volcano plot (CCNH185 vs MOD). (**D**) Cluster heat map of representative differential metabolites. The concentration changes of key metabolites (**E**) uric acid, (**F**) inosine, (**G**) xanthosine, (**H**) salicylic acid, (**I**) Prostaglandin E2 and (**J**) glutathione in serum after *L. plantarum* CCNH185 intervention. $n = 5$ mice per group. All data are presented as the mean ± S.E.M. * $p < 0.05$, ** $p < 0.01$, *** $p < 0.001$, **** $p < 0.0001$, ns, not significantly.

3.7. L. plantarum Ccnh185 Improved the Gut Microbiota Composition in HUA Mice

Metagenomic sequencing was used to analyze the structural changes of fecal flora in mice after *L. plantarum* CCNH185 intervention. Alpha diversity analysis showed that there was no significant difference in species richness between the groups ($p = 0.3175$) (Figure 7A). The beta diversity analysis based on PCoA showed that the MOD group had a significant deviation from the CK group, indicating that the high-purine diet influenced the composition of the flora. After *L. plantarum* CCNH185 intervention, there was a certain degree of change in the flora (Figure 7B). This point can also be found from the analysis of the species composition at the phylum level. After the intervention with *L. plantarum* CCNH185, the difference with the MOD group could not be observed at the gate level. However, compared with the CK group, the abundance of *Bacteroides* in the model group was significantly increased (Figure 7C). However, following *L. plantarum* CCNH185 intervention, genus-level analysis revealed increased relative abundance of *Lactiplantibacillus*, *Alistipes*, *Akkermansia*, and *Duncaniella*, along with decreased relative abundance of *Lepagella*, *Clostridium*, and *Muribaculum* (Figure 7D). Further differential bacterial analysis (Wilcoxon rank-sum test) showed that *L. plantarum* CCNH185 intervention had a clearer regulatory effect at the species level. Relative to the MOD group, *Lactiplantibacillus plantarum* and *Lactiplantibacillus* were significantly enriched. At the same time, the relative abundance of *Turicimonas muris*, *Clostridioides difficile* and *Agathobacter* significantly decreased (Figure 7E). The relative abundances of *Lactobacillus* and *Akkermansia* were positively associated with serum UA, CR, and BUN levels and with barrier protein gene expression (*ZO-1* and *Claudin-1/15*), but negatively associated with colonic *GLUT9* and *IL-1β* expression, as shown by Spearman correlation heatmap analysis. Additionally, *Lactobacillus* was also positively correlated with the expression of *ABCG2* in the ileum (Figure 7F). These results indicated that treatment with *L. plantarum* CCNH185 may mitigate murine HUA by enhancing beneficial bacterial colonization, suppressing potential pathogens, and remodeling the composition of key functional bacteria.

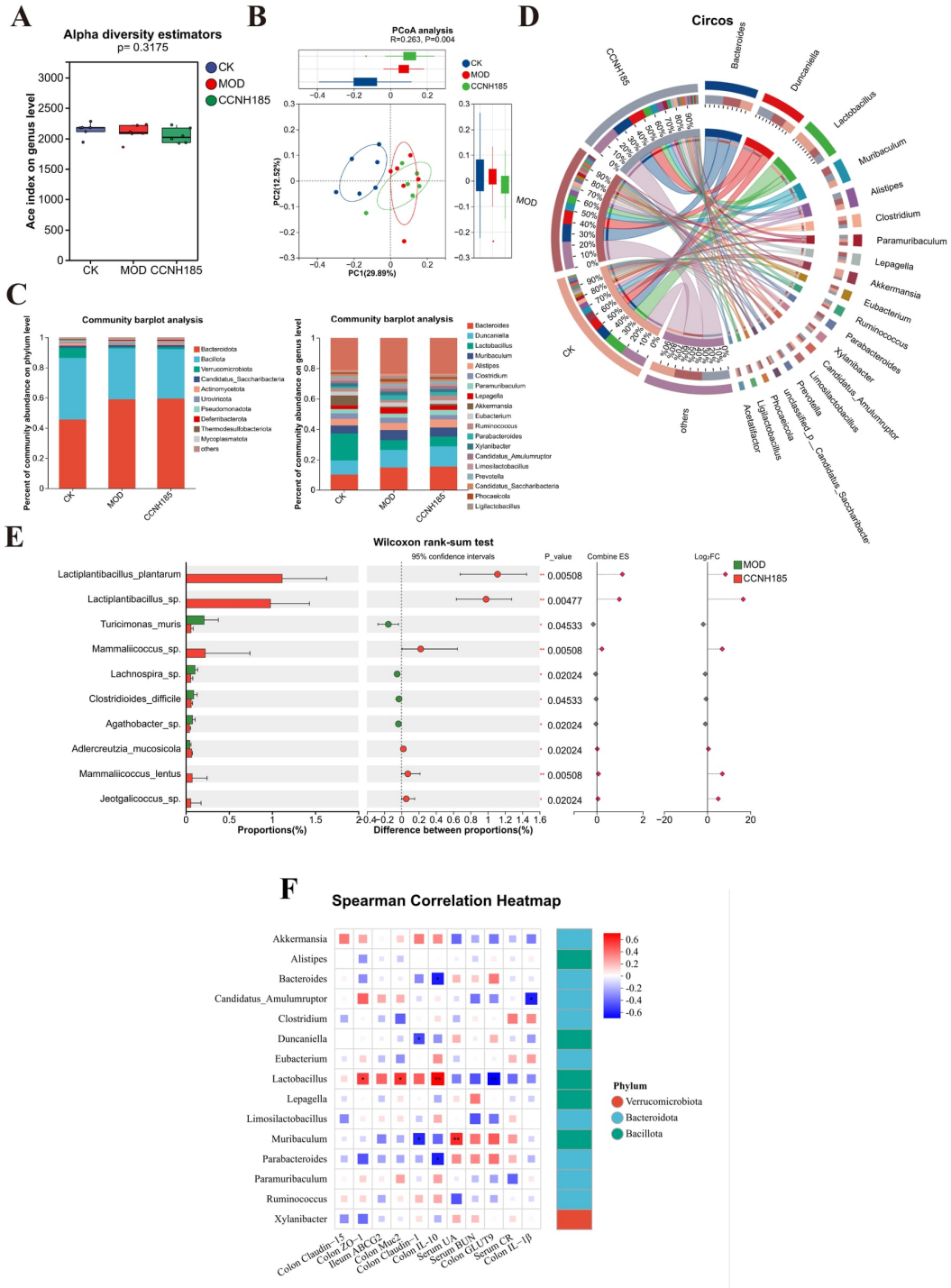

Figure 7. Effect of *L. plantarum* CCNH185 intervention on intestinal flora composition. (**A**) Ace index of Alpha diversity. (**B**) Principal coordinates analysis (PCoA) plot. (**C**) Relative abundance of microbiota at the phylum and genus level. (**D**) Circos sample-species relationship diagram at the genus level. (**E**) Species difference analysis at the species level. (**F**) Spearman correlation analysis between microbiota at the genus level and biochemical parameters. $n = 6$ mice per group. All data are presented as the mean ± S.E.M. * $p < 0.05$, ** $p < 0.01$.

4. Discussion

Foods rich in purines, such as meat and seafood, and alcoholic beverages can potently aggravate HUA. Purines are absorbed in the small intestine. As a key intermediate product of purine metabolism, nucleosides can be converted into UA by phosphorylation and oxidation in the liver [8]. As probiotics, lactic acid bacteria have been reported to have the ability

to prevent chronic disease HUA [28–30]. Probiotics can reduce the production of UA by reducing the absorption of nucleosides by the host. Rapid hydrolysis of nucleosides to nucleobases in *L. plantarum* is mediated by three ribonucleoside hydrolases, RihA- C. Since intestinal epithelial cells take up nucleobases less readily than nucleosides, this process results in decreased urate production [17]. The mouse model is an important means to explore the alleviation of HUA by probiotics. The UA oxidase gene cluster in rodents can further break down UA to allantoin; in humans, however, this enzyme became a pseudogene during early evolution and therefore lost its activity. Therefore, inhibition of its activity is a key factor in the establishment of the HUA model. Potassium oxonate can inhibit UA oxidase activity and combined with inosine and guanosine, can make UA abnormalities more obvious. After the intervention of probiotics, the CCNH185 group showed a significant decrease in serum UA levels. Therefore, *L. plantarum* has a certain ability to reduce UA [31].

Key enzymes involved in UA biosynthesis are attractive therapeutic targets for HUA, and inhibiting their activity represents a promising treatment strategy. Adenine nucleosides are metabolized to inosine under the catalysis of ADA, resulting in an increase in the content of inosine, which is then converted into UA under the catalysis of PNP and XOD. Therefore, the decrease in ADA, PNP and XOD activity is helpful in alleviating HUA. We found that *L. plantarum* CCNH185 effectively inhibited the activity and gene expression levels of key enzymes in UA synthesis in the liver of hyperuricemic mice, thereby alleviating the accumulation of purine in vivo. Increasing the excretion of UA in the kidney and intestine is also an important means to alleviate HUA. Therefore, improving the function of UA transporters to promote UA excretion is also one of the important targets for the treatment of HUA [32]. We also found that the expression of *GLUT9*, *URAT1* and *OAT1* genes returned to normal levels after supplementation with *L. plantarum* CCNH185. In addition, we also found that *L. plantarum* CCNH185 also improved the abnormal expression of *OAT3*, *ABCG2* and *NPT1*. These results reveal that *L. plantarum* CCNH185 promotes renal and intestinal UA excretion to alleviate HUA.

UA metabolism is closely linked to inflammatory responses. Elevated UA levels can activate the NLRP3 inflammasome and drive downstream inflammatory cytokine release, such as IL-1β, leading to immune cell dysregulation and low-grade chronic inflammation associated with HUA [33]. It has been reported that 17 (R) -RvD1 can reduce HUA by reducing the levels of inflammatory factors IL-1β, IL-6 and TNF [34]. *L. plantarum* CCNH185 inhibited the gene expression levels of IL-1β, IL-6 and TNF-α in the liver, and promoted the gene expression level of the anti-inflammatory factor IL-10. In addition, the levels of IL-1β and IL-10 in the intestine returned to normal, thereby alleviating the inflammatory response in the liver and intestine. HUA can cause damage to the intestinal barrier, thereby promoting the entry of harmful substances into the body's circulation. Tight junction protein is a key regulator of intestinal epithelial tight junction barrier function [35]. In this study, *L. plantarum* CCNH185 enhanced *ZO-1*, *Claudin-1*, and *Claudin-15* expression, which may be associated with the alleviation of HUA. The imbalance of intestinal flora structure may interfere with the synthesis of purine metabolic enzymes and is strongly associated with the onset of HUA and gout [36]. Previous studies have reported that *Bacteroides* abundance is significantly higher in the gut of patients with gout [37]. The significant enrichment of *Lactiplantibacillus* not only indicates the effectiveness and successful colonization of the *L. plantarum* CCNH185 intervention, but also indicates that *L. plantarum* may reshape the intestinal microecological environment by producing lactic acid, regulating intestinal pH and competitively inhibiting pathogenic bacteria. In addition, lactic acid can be converted into butyrate by butyric acid-producing bacteria in the intestine. Butyrate promotes the production of the anti-inflammatory cytokine IL-10 and its anti-inflammatory function is associated with inhibition of the NF-κB pathway [38]. In addition, it can also activate the GPR109A

receptor to exert anti-inflammatory effects [39,40]. Some studies have shown that *Akkermansia muciniphila*-derived extracellular vesicles can enhance intestinal barrier integrity by increasing epithelial expression of tight junction proteins [41], and via the AMPK signaling pathway to promote ZO-1 and occludin expression [42]. *Akkermansia muciniphila* can reduce intestinal inflammation by inhibiting the production of inflammatory molecules such as IL-8 [43]. The increased abundance of *Akkermansia* indicates that the intestinal barrier function may be enhanced, and its increase is usually positively correlated with inflammation relief. *Alistipes* is a kind of obligate anaerobic, bile-tolerant protein fermentation bacteria. *Alistipes* will preferentially use branched-chain amino acids as electron donors to produce branched-chain fatty acids [44]. The increased abundance of *Alistipes* indicates that the amino acid metabolism may be improved. The two major toxins produced by Clostridioides difficile, TcdA and TcdB, compromise intestinal epithelial integrity and provoke intestinal inflammation [45]. *Clostridioides difficile* produces toxins that cause severe intestinal inflammation, epithelial cell damage, and barrier disruption. Therefore, the decrease of potential inflammatory or conditional pathogenic bacteria such as *Clostridioides difficile*, *Clostridium* and *Turicimonas muris* suggested that *L. plantarum* CCNH185 intervention could reduce intestinal inflammatory load and endotoxin pressure. This study has several limitations. The microbiota shifts observed here were correlative and do not establish that they mediate the improvement in HUA. Functional validation using fecal microbiota transplantation, gnotobiotic mice, metagenomic functional prediction and microbiota-derived metabolite analysis is needed to confirm the causal role of the microbiota in the effects of CCNH185. The sample size ($n = 6$ per group) was modest and may limit the detection of small effect sizes. Only male mice were used; therefore, the findings may not be directly generalizable to female animals, and extrapolation to humans warrants further validation. An allopurinol or febuxostat positive control group was not established in this study; therefore, the efficacy of CCNH185 relative to established anti-hyperuricemic drugs cannot be assessed. Future studies should include a positive control and dose –response design to evaluate comparative efficacy.

5. Conclusions

In summary, *L. plantarum* CCNH185 with high nucleoside degradation activity effectively alleviated HUA in mice. CCNH185 inhibited the activity and expression of key UA synthesis enzymes (XOD, PNP and ADA) in the liver, thereby reducing UA production. It also promoted UA excretion by down-regulating the expression of the UA reabsorption transporter *GLUT9* in the kidney and intestine, up-regulating the expression of ABCG2 in the kidney and intestine, and UA secretion-related transporters *OAT1*, *OAT3* and *NPT1* in the kidney. Moreover, CCNH185 repaired intestinal barrier damage by increasing *ZO-1*, *Claudin-1*, *Claudin-15* and *Muc2* expression, and reduced pro-inflammatory cytokines in the intestine and liver. Targeted metabolomics revealed that CCNH185 decreased serum inosine and xanthosine, while increasing salicylic acid and glutathione, contributing to anti-inflammatory and anti-oxidative effects. CCNH185 also regulates the structure of the gut microbiota. These findings indicate that *L. plantarum* CCNH185 alleviates HUA through a multi-target mechanism, and may serve as a promising probiotic for dietary intervention of HUA. Future research should validate its efficacy in humans and elucidate the molecular basis of its interactions with host UA metabolism.

Author Contributions: Conceptualization, Y.N.; methodology, C.F., Z.Z. and J.H.; validation, Y.N.; formal analysis, Y.N., C.F. and J.Y.; investigation, C.F.; resources, J.Y.; data curation, Y.N.; writing—original draft preparation, Y.N.; writing—review and editing, Z.Z. and Y.H.; supervision, J.H.; project administration, X.Z. and Y.H.; funding acquisition, X.Z. and Y.H. All authors have read and agreed to the published version of the manuscript.

Funding: This research was funded by COFCO Corporation through the Strategic Forward-Looking-2024 "Development and Application of Key Technologies for Microbial Germplasm Resource Mining", Project Code: 2024-C1-F002.

Institutional Review Board Statement: The animal study protocol was approved by the Institutional Review Board of China Agricultural University Institutional Animal Care and Use Committee (protocol code Aw52905202-5-2, approval date 24 September 2025).

Informed Consent Statement: Not applicable.

Data Availability Statement: The original contributions presented in this study are included in the article. Further inquiries can be directed to the corresponding author.

Acknowledgments: We thank the Department of Nutrition and Health at China Agricultural University for experimental support. We also appreciate the assistance of all lab members in animal experiments and sample analysis.

Conflicts of Interest: Author Juan Yang was employed by COFCO Nutrition & Health Research Institute, COFCO Corporation, Beijing, China. She participated in formal analysis and resources in the study. Author Jiahao Huang was employed by COFCO Nutrition & Health Research Institute, COFCO Corporation, Beijing, China. He participated in the methodology and supervision of the study. Author Xiaowei Zheng was employed by COFCO Nutrition & Health Research Institute, COFCO Corporation, Beijing, China. He participated in project administration and funding acquisition in the study. The remaining authors declare that the research was conducted in the absence of any commercial or financial relationships that could be construed as a potential conflict of interest.

References

1. Li, L.; Zhang, Y.; Zeng, C. Update on the Epidemiology, Genetics, and Therapeutic Options of Hyperuricemia. *Am. J. Transl. Res.* **2020**, *12*, 3167–3181.
2. Kuo, C.-F.; Grainge, M.J.; Zhang, W.; Doherty, M. Global Epidemiology of Gout: Prevalence, Incidence and Risk Factors. *Nat. Rev. Rheumatol.* **2015**, *11*, 649–662. [CrossRef]
3. Sun, M.; Lyu, Z.; Wang, C.; Li, Y.; Zhao, D.; Ran, X.; Chen, H.; Su, B.; Chang, X.; Liu, P.; et al. 2024 Update of Chinese Guidelines for Diagnosis and Treatment of Hyperuricemia and Gout Part I: Recommendations for General Patients. *Int. J. Rheum. Dis.* **2025**, *28*, e70375. [CrossRef]
4. Zhang, M.; Zhu, X.; Wu, J.; Huang, Z.; Zhao, Z.; Zhang, X.; Xue, Y.; Wan, W.; Li, C.; Zhang, W.; et al. Prevalence of Hyperuricemia among Chinese Adults: Findings from Two Nationally Representative Cross-Sectional Surveys in 2015-16 and 2018–19. *Front. Immunol.* **2021**, *12*, 791983. [CrossRef]
5. Yokose, C.; McCormick, N.; Choi, H.K. Dietary and Lifestyle-Centered Approach in Gout Care and Prevention. *Curr. Rheumatol. Rep.* **2021**, *23*, 51. [CrossRef]
6. Perez-Ruiz, F.; Becker, M.A. Inflammation: A Possible Mechanism for a Causative Role of Hyperuricemia/Gout in Cardiovascular Disease. *Curr. Med. Res. Opin.* **2015**, *31*, 9–14. [CrossRef]
7. Chen, M.-Q.; Wang, H.-Y.; Shi, W.-R.; Sun, Y.-X. Estimate of Prevalent Hyperuricemia by Systemic Inflammation Response Index: Results from a Rural Chinese Population. *Postgrad. Med.* **2021**, *133*, 242–249. [CrossRef]
8. Maiuolo, J.; Oppedisano, F.; Gratteri, S.; Muscoli, C.; Mollace, V. Regulation of Uric Acid Metabolism and Excretion. *Int. J. Cardiol.* **2016**, *213*, 8–14, Correction in *Int. J. Cardiol.* **2023**, *387*, 131126. [CrossRef]
9. Chaudhary, K.; Malhotra, K.; Sowers, J.; Aroor, A. Uric Acid—Key Ingredient in the Recipe for Cardiorenal Metabolic Syndrome. *Cardiorenal Med.* **2013**, *3*, 208–220. [CrossRef]
10. Mandal, A.K.; Mount, D.B. The Molecular Physiology of Uric Acid Homeostasis. *Annu. Rev. Physiol.* **2015**, *77*, 323–345. [CrossRef]
11. Otani, N.; Ouchi, M.; Misawa, K.; Hisatome, I.; Anzai, N. Hypouricemia and Urate Transporters. *Biomedicines* **2022**, *10*, 652. [CrossRef]
12. Siu, Y.-P.; Leung, K.-T.; Tong, M.K.-H.; Kwan, T.-H. Use of Allopurinol in Slowing the Progression of Renal Disease through Its Ability to Lower Serum Uric Acid Level. *Am. J. Kidney Dis. Off. J. Natl. Kidney Found.* **2006**, *47*, 51–59. [CrossRef]
13. Keenan, R.T.; Pillinger, M.H. Febuxostat: A New Agent for Lowering Serum Urate. *Drugs Today* **2009**, *45*, 247–260. [CrossRef]
14. Nyberg, M.; Piil, P.; Kiehn, O.T.; Maagaard, C.; Jørgensen, T.S.; Egelund, J.; Isakson, B.E.; Nielsen, M.S.; Gliemann, L.; Hellsten, Y. Probenecid Inhibits α-Adrenergic Receptor-Mediated Vasoconstriction in the Human Leg Vasculature. *Hypertension* **2018**, *71*, 151–159. [CrossRef]

15. Ishikawa, T.; Maeda, T.; Hashimoto, T.; Nakagawa, T.; Ichikawa, K.; Sato, Y.; Kanno, Y. Long-Term Safety and Effectiveness of the Xanthine Oxidoreductase Inhibitor, Topiroxostat in Japanese Hyperuricemic Patients with or without Gout: A 54-Week Open-Label, Multicenter, Post-Marketing Observational Study. *Clin. Drug Investig.* **2020**, *40*, 847–859. [CrossRef]
16. Ni, C.X. Study of the Effects and Approaches of Lactobacillus on Hyperuricaemia Alleviation. Master's Thesis, Jiangnan University, Wuxi, China, 2021. (In Chinese)
17. Li, M.; Wu, X.; Guo, Z.; Gao, R.; Ni, Z.; Cui, H.; Zong, M.; Van Bockstaele, F.; Lou, W. *Lactiplantibacillus plantarum* Enables Blood Urate Control in Mice through Degradation of Nucleosides in Gastrointestinal Tract. *Microbiome* **2023**, *11*, 153. [CrossRef]
18. Wang, Z.; Huang, Y.; Yang, T.; Song, L.; Xiao, Y.; Chen, Y.; Chen, M.; Li, M.; Ren, Z. *Lactococcus cremoris* D2022 Alleviates Hyperuricemia and Suppresses Renal Inflammation via Potential Gut-Kidney Axis. *Food Funct.* **2024**, *15*, 6015–6027. [CrossRef]
19. Zhao, H.; Chen, X.; Zhang, L.; Meng, F.; Zhou, L.; Pang, X.; Lu, Z.; Lu, Y. *Lacticaseibacillus rhamnosus* Fmb14 Prevents Purine Induced Hyperuricemia and Alleviate Renal Fibrosis through Gut-Kidney Axis. *Pharmacol. Res.* **2022**, *182*, 106350. [CrossRef]
20. Wang, Q.; Liang, J.; Zou, Q.; Wang, W.; Yan, G.; Guo, R.; Yuan, T.; Wang, Y.; Liu, X.; Liu, Z. Tryptophan Metabolism-Regulating Probiotics Alleviate Hyperuricemia by Protecting the Gut Barrier Integrity and Enhancing Colonic Uric Acid Excretion. *J. Agric. Food Chem.* **2024**, *72*, 26746–26761. [CrossRef]
21. Jing, Y.; Bai, X.; Yin, Y.; Liu, X.; Li, J.; Chen, Z.; Zhai, Z.; Hao, Y. *Lactiplantibacillus plantarum* CCNH185 Attenuates *Citrobacter rodentium*-Induced Colitis by Reshaping Gut Microbiota Structure and Modulating Innate Immunity. *Foods* **2026**, *15*, 1815. [CrossRef]
22. Xiao, Y.; Zhang, C.; Zeng, X.; Yuan, Z. Microecological Treatment of Hyperuricemia Using Lactobacillus from Pickles. *BMC Microbiol.* **2020**, *20*, 195. [CrossRef]
23. Jing, Y.; Bai, X.; Qian, H.; Wang, Y.; Hao, Y.; Zhai, Z.; Zhang, Z.; Hao, Y. *Limosilactobacillus reuteri* Urob-7 Alleviates Hyperuricemia by Modulating Uric Acid Metabolism through Nucleoside Degradation and Xanthine Oxidase Inhibition. *Foods* **2025**, *14*, 3706. [CrossRef]
24. Zhou, H.; Zhao, X.; Ye, D.; Zhao, Q.; Yang, M.; Wang, Z.; Wang, L.; Wang, C.; Geng, S.; Zeng, W.; et al. Salicylic Acid Inhibits Mas-Related G Protein-Coupled Receptor X2-Mediated Mast Cell 2 Activation and Mitigates Cutaneous Pseudo-Allergic Reactions. *Eur. J. Pharmacol.* **2025**, *1006*, 178189, Correction in *Eur. J. Pharmacol.* **2025**, *1007*, 178247. [CrossRef]
25. Kaushal, K.; Goutam, N.; Sharma, A. Shivani Phytotherapeutic Insights into Hyperuricemia: A Mechanistic and Clinical Perspective. *Inflammopharmacology* **2025**, *33*, 4335–4354. [CrossRef]
26. Carlin, G.; Djursäter, R.; Smedegård, G.; Gerdin, B. Effect of Anti-Inflammatory Drugs on Xanthine Oxidase and Xanthine Oxidase Induced Depolymerization of Hyaluronic Acid. *Agents Actions* **1985**, *16*, 377–384. [CrossRef]
27. Furuhashi, M. New Insights into Purine Metabolism in Metabolic Diseases: Role of Xanthine Oxidoreductase Activity. *Am. J. Physiol. Endocrinol. Metab.* **2020**, *319*, E827–E834. [CrossRef]
28. Cao, T.; Li, X.; Mao, T.; Liu, H.; Zhao, Q.; Ding, X.; Li, C.; Zhang, L.; Tian, Z. Probiotic Therapy Alleviates Hyperuricemia in C57BL/6 Mouse Model. *Biomed. Res.-India* **2017**, *28*, 2244–2249.
29. Yamada, N.; Saito-Iwamoto, C.; Nakamura, M.; Soeda, M.; Chiba, Y.; Kano, H.; Asami, Y. Lactobacillus Gasseri PA-3 Uses the Purines IMP, Inosine and Hypoxanthine and Reduces Their Absorption in Rats. *Microorganisms* **2017**, *5*, 10. [CrossRef]
30. Wang, H.; Mei, L.; Deng, Y.; Liu, Y.; Wei, X.; Liu, M.; Zhou, J.; Ma, H.; Zheng, P.; Yuan, J.; et al. Lactobacillus Brevis DM9218 Ameliorates Fructose-Induced Hyperuricemia through Inosine Degradation and Manipulation of Intestinal Dysbiosis. *Nutrition* **2019**, *62*, 63–73. [CrossRef]
31. Fu, Y.; Luo, X.-D.; Li, J.-Z.; Mo, Q.-Y.; Wang, X.; Zhao, Y.; Zhang, Y.-M.; Luo, H.-T.; Xia, D.-Y.; Ma, W.-Q.; et al. Host-Derived Lactobacillus Plantarum Alleviates Hyperuricemia by Improving Gut Microbial Community and Hydrolase-Mediated Degradation of Purine Nucleosides. *eLife* **2024**, *13*, e100068. [CrossRef]
32. Tátrai, P.; Erdő, F.; Dörnyei, G.; Krajcsi, P. Modulation of Urate Transport by Drugs. *Pharmaceutics* **2021**, *13*, 899. [CrossRef]
33. Li, D.; Yuan, S.; Deng, Y.; Wang, X.; Wu, S.; Chen, X.; Li, Y.; Ouyang, J.; Lin, D.; Quan, H.; et al. The Dysregulation of Immune Cells Induced by Uric Acid: Mechanisms of Inflammation Associated with Hyperuricemia and Its Complications. *Front. Immunol.* **2023**, *14*, 1282890. [CrossRef]
34. Zhao, L.; Zhang, Y.; Qiao, Y.; Jia, L.; Luo, S. 17(R)-RvD1 Ameliorates Liver Injury in Hyperuricemia through Inhibiting Pyroptosis via NF-κB Signaling Pathway. *Drug Des. Devel. Ther.* **2025**, *19*, 6573–6585. [CrossRef]
35. Zuo, L.; Kuo, W.-T.; Turner, J.R. Tight Junctions as Targets and Effectors of Mucosal Immune Homeostasis. *Cell. Mol. Gastroenterol. Hepatol.* **2020**, *10*, 327–340. [CrossRef]
36. Zhao, H.; Lu, Z.; Lu, Y. The Potential of Probiotics in the Amelioration of Hyperuricemia. *Food Funct.* **2022**, *13*, 2394–2414. [CrossRef]
37. Shao, T.; Shao, L.; Li, H.; Xie, Z.; He, Z.; Wen, C. Combined Signature of the Fecal Microbiome and Metabolome in Patients with Gout. *Front. Microbiol.* **2017**, *8*, 268. [CrossRef]
38. Zhao, Y.; Chen, J.; Qin, Y.; Yuan, J.; Yu, Z.; Ma, R.; Liu, F.; Zhao, J. Linking Short-Chain Fatty Acids to Systemic Homeostasis: Mechanisms, Therapeutic Potential, and Future Directions. *J. Nutr. Metab.* **2025**, *2025*, 8870958. [CrossRef]

39. Leko, L.; Simic, D.; Martins, T.V.; da Silva, G.V.L.; Maillet, I.; Savigny, F.; Vuksan, L.; Rodrigues, D.d.M.; Le Bert, M.; Offermanns, S.; et al. Butyrate Receptor HCAR2/GPR109A Controls Imiquimod-Induced Psoriasis-like Skin Inflammation. *J. Immunol.* **2025**, *214*, 2029–2040. [CrossRef]
40. Shao, X.; Mi, X.; Kuai, X.; Zhou, D.; Tai, Q.; Lu, Y.; Zhou, C.; He, S. Microbial Butyrate Modified by Melatonin Alleviates Colon Inflammation by Inhibiting GPR109A/Caspase-1-Dependent Macrophage M1 Polarization. *J. Proteome Res.* **2025**, *24*, 1871–1884. [CrossRef]
41. Ghaderi, F.; Hajebrahimi, Z.; Fateh, A.; Sotoodehnejadnematalahi, F.; Ahmadi Badi, S.; Vaezijoze, S.; Siadat, S.D. Tight Junctions Expression Is Affected by Active, Inactive, and Derivatives of *Akkermansia muciniphila*. *Iran. J. Microbiol.* **2025**, *17*, 885–892. [CrossRef]
42. Wang, Y.; Sun, Z.; Wang, L.; Shi, H.; Xiao, S.; Dong, F.; Qin, N. Therapeutic Application of Probiotic Extracellular Vesicles in Inflammatory Bowel Disease. *J. Adv. Res.* 2026; *in press*. [CrossRef]
43. Pan, M.; Barua, N.; Ip, M. Mucin-Degrading Gut Commensals Isolated from Healthy Faecal Donor Suppress Intestinal Epithelial Inflammation and Regulate Tight Junction Barrier Function. *Front. Immunol.* **2022**, *13*, 1021094. [CrossRef]
44. Wolf, P.G.; Byrd, D.A.; Cares, K.; Dai, H.; Odoms-Young, A.; Gaskins, H.R.; Ridlon, J.M.; Tussing-Humphreys, L. Bile Acids, Gut Microbes, and the Neighborhood Food Environment-a Potential Driver of Colorectal Cancer Health Disparities. *mSystems* **2022**, *7*, e0117421. [CrossRef]
45. Brayan, M.-T.; Alejandro, A.-A.; Quesada-Gómez, C.; Chaves-Olarte, E.; Elías, B.-C. Polymorphonuclear Neutrophil Depletion in Ileal Tissues Reduces the Immunopathology Induced by *Clostridioides Difficile* Toxins. *Anaerobe* **2025**, *92*, 102947. [CrossRef]

Disclaimer/Publisher's Note: The statements, opinions and data contained in all publications are solely those of the individual author(s) and contributor(s) and not of MDPI and/or the editor(s). MDPI and/or the editor(s) disclaim responsibility for any injury to people or property resulting from any ideas, methods, instructions or products referred to in the content.